

STUDIES OF RESONANT SYNCHROTRON OSCILLATION EFFECTS USING MOSER TRANSFORMATIONS\*

J. D. Steben, H. K. Meier, and K. R. Symon  
Midwestern Universities Research Association  
Stoughton, Wisconsin

Summary

Nonlinear synchrotron oscillations are present in virtually all accelerators (for economic reasons). For RF parameters likely to be used in 600-1000 GeV accelerators, or in high frequency (high harmonic) RF systems at lower energies, these nonlinearities give rise to numerous resonances, including basic noncoupled resonances which the present study investigates both by analytical and computational methods. A relatively simple theory<sup>1</sup> has been sufficient to explain qualitatively many effects, such as "propellers" and "beads" in phase space, for both third- and half-integral resonances. Some extensions of the work of reference 1 are reported. However, understanding some details of the  $\nu = \frac{1}{4}$  resonance was not possible without the use of Moser transformations.<sup>2</sup> In particular, a null occurs in the resonance driving term as the synchronous particle phase  $\Phi_s$  is varied, an effect predicted by the Moser theory. Our results indicate that suitably designed particle accelerators may operate in the vicinity of some phase oscillation resonances but that the resonances in question influence the desirable choice of  $\Phi_s$ .

A. Introduction

In most conventional treatments of particle motion in accelerators, the expression

$$\nu_s \equiv \sqrt{\frac{hK V \cos \Phi_s}{2\pi E_s}}, \quad K \equiv \frac{E}{F} \frac{df}{dE} \quad (1)$$

where  $\Gamma \equiv \sin \Phi_s$  is the fraction of the maximum possible energy gain  $V$  per turn<sup>1</sup> which is needed for a particle to remain synchronous (all notation agrees with Ref. 1), is used for the frequency of phase oscillations, taken to be small compared to unity and to betatron oscillation frequencies. This is not an exceptionally good approximation for some present-day accelerators which obtain values  $\nu_s \approx 0.05$ , and may fail completely at the higher energies (200-1000 GeV) envisioned in the next "generation" of accelerators. The maximum  $\nu_s$  attained during the acceleration cycle (above transition) is roughly

$$\nu_{s,max} = \sqrt{\frac{hV(-\cos \Phi_s)}{3\sqrt{3}\pi E_0 \nu_r^3}}, \quad (2)$$

attained at roughly  $3\gamma_T$ , where  $\gamma_T E_0$  is the transition energy.

As  $\nu_{s,max}$  is comparable with unity for the highest energy and/or frequency accelerators currently under consideration, resonances will undoubtedly be crossed and resonant effects may become important and limit stability. This was shown in Ref. 1, as well as the fact that the synchrotron oscillation frequency for an accelerator with any periodicity  $N$  of evenly spaced RF gaps is given not by  $\nu_s$  but by  $\nu_s(\nu_s)$ , where

$$\cos \frac{2\pi\nu_s}{N} = 1 - \frac{1}{2} \left( \frac{2\pi\nu_s}{N} \right)^2 \quad (3)$$

The Hamiltonian of the motion about the synchronous phase  $\Phi_s$  and energy  $E_s$  was given by

$$H(\varphi, y, \tau) = \frac{y^2}{2} + \nu_s^2 \left[ 2 \sin^2 \frac{\varphi}{2} - \tan \Phi_s (\varphi - \sin \varphi) \right] \cdot \left[ 1 + 2 \sum \cos_j N\tau + 2\epsilon \sum_{m=1}^{\infty} \cos m\tau \right] \quad (4)$$

where

$$y = -\frac{hK}{E_s}(E - E_s), \quad \varphi = \Phi - \Phi_s, \quad \tau = 2\pi f_s t, \quad (5)$$

$\Phi$  being the phase of the RF gap when the particle passes it ( $\varphi = y = 0$  for the synchronous particle). In the limit  $\nu_s \ll 1$ , the time dependence of  $H$  becomes of negligible importance, and one obtains the conventional "bucket area," given<sup>3</sup> by

$$A_s = 16 \nu_s \alpha(\Gamma) = 16 \alpha_s(\Gamma) \sqrt{\frac{h|K|V}{2\pi E_s}} \quad (6)$$

in  $y$ - $\varphi$  units.

From this point, in the approximate theory the Hamiltonian was transformed to canonical polar coordinate

$$\gamma = \cos^{-1} \frac{y}{\varphi} \quad \text{and} \quad \rho = \frac{y^2}{2\nu_s} + \nu_s \frac{\varphi^2}{2}$$

giving  $H = \nu_s \rho + \dots$  and an approximate nonlinear Hamiltonian was assumed with a central part

\*Work performed under the auspices of the U. S. Atomic Energy Commission.

$$H_c = \nu_c \rho_c \frac{1}{1 + \frac{\epsilon}{\Gamma}} \left[ 1 - \frac{\rho}{\rho_c} \right]^{1 + \frac{\epsilon}{\Gamma}}, \quad \rho_c = \frac{A_s}{2\pi}, \quad (7)$$

where

$$\nu_c(\rho) = \frac{\partial H}{\partial \rho} = \frac{d\nu}{d\rho} = \nu_0 \left[ 1 - \frac{\rho}{\rho_c} \right]^{\frac{\epsilon(\Gamma)}{\Gamma}} \quad (8)$$

was correctly matched near  $\rho = 0$  (ignoring non-resonant time dependence), and the  $\frac{m}{n}$  resonance was then made stationary by going to rotating coordinates  $\underline{\rho} = \rho$  and  $\underline{\chi} = \chi - \frac{m\Gamma}{n}$ , so

$$\underline{H} = H - \frac{m}{n} \rho \quad (9)$$

and the resonant part derived from Eq. (4) became

$$\underline{H}_{(\nu = \frac{1}{n})} = \frac{\epsilon}{n!} 2^{1 - \frac{n}{2}} \rho^{\frac{n}{2}} \nu_c^{2 - \frac{n}{2}} \left\{ \begin{matrix} \tan \underline{\Phi}_s, \sin 4\underline{\chi} \\ - \cos n\underline{\chi} \end{matrix} \right\} \dots \quad (10)$$

in the lowest order.  $\left\{ \begin{matrix} n \text{ odd} \\ n \text{ even} \end{matrix} \right\}$

While the preceding approximate theory was quite useful, it is accurate (topologically) only to first order in  $\tan \underline{\Phi}_s$ . The more thorough basic theory developed by Moser<sup>2</sup> (as an extension of earlier work<sup>4</sup>) corrects this deficiency, giving more accurate predictions (even qualitatively, for the resonance  $\nu_c = \frac{1}{4}$ ). The Moser transformations generate a formal solution to the problem and this is carried out to quartic ( $\rho^2$ ) order in Section C.

B. Extensions of Simpler Treatment of Resonances

Application of the simpler theory is quite beneficial for understanding the half-integral resonance. Referring to Figs. 6 and 8 in Ref. 1, the Hamiltonian

$$H = (\nu_c - \frac{1}{2})\rho - \frac{\rho^2}{16} - \frac{\epsilon \nu_c \rho}{2} \cos 2\underline{\chi} + \frac{\epsilon \rho^2}{12} \cos 2\underline{\chi} \quad (11)$$

gives the correct linear stopband

$$\frac{1}{2 + |\epsilon|} < \nu_c < \frac{1}{2 - |\epsilon|}$$

and predicts the observed larger amplitude stability, for  $|\epsilon| < 1$ , but not for  $\epsilon = 1$  where an absolute upper frequency cutoff is encountered, at  $\nu_s = \frac{1}{\Gamma}$ , rather than just a "stopband." Theory and experiment also agree as to the variation of the observed propeller size with  $\nu_c$  and  $\epsilon$ .

The propeller increases from zero size at

$\nu = \frac{1}{2 + |\epsilon|}$  to maximum size at  $\frac{1}{2 - |\epsilon|}$  with an area

$$A_p = 16 \left\{ \epsilon \nu_c \sqrt{1 - \left( \frac{2\nu_c - 1}{|\epsilon| \nu_c} \right)^2} + (2\nu_c - 1) \left[ \pi - \cos^{-1} \left( \frac{2\nu_c - 1}{|\epsilon| \nu_c} \right) \right] \right\}, \quad (12)$$

$|\epsilon| < 1$

which becomes  $A_p = 8\epsilon$  (directly proportional to the imperfection signal) at  $\nu_c = \frac{1}{2}$  (by contrast the propeller area varies as  $\epsilon^2$  at  $\nu_c = \frac{1}{3}$ ). Below the  $\nu_c = \frac{1}{2}$  imperfection resonance, topology is normal, but above it, beads occur, as shown in Fig. 8 of Ref. 1. Areas of the propellers and beads are tabulated at the end of this section.

In the previous paper we established that the effects of the  $\nu_c = \frac{1}{3}$  resonance could be made small for an imperfection resonance but always followed the same pattern, namely petals, propellers, and beads (Fig. 2 of Ref. 1). We have investigated computationally and theoretically the dependence of this resonance (for  $\Gamma \approx 0.6$ ,  $|\epsilon| \ll 1$  it becomes as strongly driven as the corresponding half-integral resonance) and will discuss in Part D the conditions under which the propellers or beads, for the intrinsic ( $\epsilon = 1$ ) case become "detached" and degenerate into "islands of stability."

We may drop terms of higher order than  $\rho^4$  in the expansion of Eq. (7), to investigate the topology of the quarter-integral resonance near  $\rho = 0$ . Using Eq. (9) we then obtain

$$\underline{H} = (\nu_c - \frac{1}{4})\rho - \frac{\rho^2}{16} - \frac{\rho^2}{48} \cos 4\underline{\chi} \quad (13)$$

This Hamiltonian implies that no petals or propeller will form (i. e., normal topology at  $\nu_c \leq \frac{1}{4}$ ), as differentiating  $\underline{H}$  with respect to  $\rho$  and  $\underline{\chi}$  yields stationary or fixed points at

$$(\rho, \underline{\chi}) = \left( \frac{8(\nu_c - \frac{1}{4})}{1 - \frac{\epsilon}{3}}, (n + \frac{1}{4} \pm \frac{1}{4}) \frac{\pi}{2} \right) \quad (14)$$

where the bead centers (upper possibilities in Eq. (14) iff  $\epsilon > 0$ ) always occur for the larger  $\rho$  value and the unstable fixed points (saddle points of H) occur at the smaller  $\rho$  in (14). Actually the dependence of all  $\rho^2$  coefficients involves additional terms containing the factor

$$\tan^2 \underline{\Phi}_s = \frac{\Gamma^2}{1 - \Gamma^2},$$

but topologically the conclusions above have been correct, for  $\Gamma \lesssim 0.7$ .

The simple theory (first order in  $\tan \underline{\Phi}_s$ ) fails to predict a null (and change in bead position) in the resonance as  $\Gamma$  is increased, an effect observable in Fig. 2. This prediction occurs, however, in the more accurate Moser transformation treatment to be described in the following section.

Similar (less accurate) statements could be made about the  $\nu_c = \frac{1}{5}$  resonance, for which Moser transformations are even more essential.

Area predictions of the above theory for the variation of resonant phase space areas (propellers and beads) with  $\nu_0$ ,  $\epsilon$ , and  $\Gamma$  (but only for  $\Gamma \ll 1$ ) seem well verified (for  $\rho \ll \rho_c$ ) and are summarized in the following table of areas:

$\nu_0$	Propeller Area	Area in Beads
$\frac{1}{2}$	$8 \epsilon $ at $\nu_0 = \frac{1}{2}$	$16 \left[ \pi \left( \nu_0 - \frac{1}{2} \right) - \sqrt{(2\nu_0 - 1 +  \epsilon  \nu_0)} + (2\nu_0 - 1) \sin^{-1} \sqrt{\frac{ \epsilon  \nu_0}{2\nu_0 - 1}} \right]$
$\frac{1}{3}$	$\approx \epsilon^2 \tan^2 \bar{\Phi}_s$	
$\frac{1}{4}$	0	$\approx 8 \epsilon  \left( \nu_0 - \frac{1}{4} \right)$

in the  $(\varphi, y)$  units used above.

C. Moser Transformation of the Motion

The Moser transformations successively remove the time dependence from H to higher orders in  $\rho$ . The "linear" transformation (using Floquet solutions) changes it to the form<sup>5</sup>

$$H = \nu_0 \rho + \left[ -\frac{\nu_0^{3/2} \sqrt{2} \epsilon \tan \bar{\Phi}_s}{24 (\cos \frac{\pi \nu_0}{N})^{3/4}} \rho^3 \sin^3 \gamma - \frac{\epsilon}{96 \cos \frac{\pi \nu_0}{N}} \rho^2 \sin^4 \gamma + \frac{\sqrt{2} \epsilon \nu_0^{1/2} \tan \bar{\Phi}_s \rho^5 \sin^5 \gamma}{960 (\cos \frac{\pi \nu_0}{N})^{5/4}} \right] \cdot \left[ 1 + 2 \sum_{m=1}^{\infty} \epsilon_m \cos m\tau \right], \quad \epsilon_m = \epsilon + (1-\epsilon) \delta_{m,jN} \quad (15)$$

j: any integer

The third order transformation (which was done in complex coordinates  $\bar{y} = \sqrt{\rho} e^{i\gamma}$  and  $\bar{z}_3 = \sqrt{\rho_3} e^{-i\gamma_3}$ , as a convenient though unnecessary generalization of the usual canonical transformation) was generated by

$$S_F = \bar{y} \bar{z}_3 + \sum_{k+l=3} S_{k,l} \bar{y}^k \bar{z}_3^l + \frac{i}{2} \sum_{k+l=3} \sum_{k'+l'=3} S_{k,l}^{(3)} S_{k',l'}^{(3)} \bar{y}^{k+k'} \bar{z}_3^{l+l'} \quad (16)$$

where

$$iH_3 = \Omega_3 = \Omega + \frac{\partial S_F}{\partial \bar{z}_3}, \quad \Omega = iH \quad (17)$$

is used to completely remove the  $\rho^{3/2} \cos(m\gamma) e^{im\tau}$  terms from H (for  $\nu_0 < \frac{1}{3}$ ), where

$$S_{k,l} = \sum S_{k,l,m} e^{im\tau}, \quad S_{k,l,m} = \frac{\sqrt{2} \nu_0^{1/2} \epsilon_m \tan \bar{\Phi}_s i^{(k-l)}}{4 [\nu_0 (k-l) - m] \left[ \cos \frac{\pi \nu_0}{N} \right]^{3/4}} \quad (18)$$

producing

$$H_3 = \nu_0 \rho_3 + \left( W_{22} + \frac{1}{2} W_{3003} + \frac{3}{2} W_{2112} + C_{2112} \right) \rho^2 + \left( W_{13} + 3W_{2103} + C_{2103} \right) \rho^2 \sin^2 \gamma + \left( W_{04} + \frac{3}{2} W_{1203} \right) \rho^2 \sin^4 \gamma \quad (19)$$

where  $W_{k,l}$ ,  $W_{k,l,k'}$  and  $C_{k,l,k'}$  are functions of  $\tau$  defined by

$$W_{k,l} = \sum_{m=-\infty}^{\infty} W_{k,l,m} e^{im\tau} = - \sum_{m=1}^{\infty} \frac{e^{im\tau}}{64 k! l! \cos \frac{\pi \nu_0}{N}}$$

$$C_{k,l,k'} = 2 \nu_0 S_{k,l} S_{k',l'} e^{i(k+l-k')\tau}$$

$$W_{k,l,k'} = C_{k,l,k'} - W_{k,l} S_{k',l'} e^{i(k+l-k')\tau} + W_{k',l'} S_{k,l} e^{i(k+l-k')\tau} \quad (20)$$

As  $W_{k,l}$  and  $S_{k,l}$  contain the factor  $\tan \bar{\Phi}_s$ , all of the  $W_{k,l,k'}$  and  $S_{k,l,k'}$  terms contain  $\tan^2 \bar{\Phi}_s = \frac{\Gamma^2}{1-\Gamma^2}$  as a factor. Similarly, the fourth order Moser transformation eliminates all of the nonresonant  $\tau$  dependence from  $\rho^2$  terms. We may then apply the transformation (9) (with  $m = 1, n = 4$ ) to rotating coordinates, obtaining

$$H_4 = \left( \nu_0 - \frac{1}{4} \right) \rho_4 + \left( W_{220} + \frac{9}{2} W_{30030} + \frac{3}{2} W_{21120} + C_{21120} \right) \rho_4^2 + \left( 2W_{041} + 3W_{12031} \right) \rho_4^2 \cos(4\gamma_4) \quad (21)$$

where  $W_{k,l,k',m}$  and  $S_{k,l,k',m}$  satisfy relationships of the form

$$W_{k,l,k',m} = \sum_{m'=-\infty}^{\infty} W_{k,l,k',m'} e^{im'\tau}, \quad W_{k,l,k',m} = W_{k',l',k,-m}$$

Evaluation of the coefficient  $(2W_{041} + 3W_{12031})$  in (21) indicates that  $W_{12031}$  is of the form

$2W_{041} \left[ 1 - \tan^2 \bar{\Phi}_s \left( a + \frac{b}{\frac{1}{3} - \nu_0} \right) \right]$  where  $a(\nu_0)$  and  $b(\nu_0)$  are positive slowly varying functions, correctly predicting the null in the driving term (but the coefficient of  $\tan^2 \bar{\Phi}_s$  is too small for good numerical agreement with computations). While a similar effect in the central term could possibly produce changes in the topology for  $\nu_0 \leq \frac{1}{4}$ , computations indicate the  $w_{220}$  part is dominant, at least for  $\Gamma \leq 0.7$ , so the topology is normal below and at  $\nu_0 = \frac{1}{4}$ .

It might be noted that a similar study of the  $\nu_0 = \frac{1}{5}$  resonance (which is relatively minor except if  $\tan \bar{\Phi}_s$  is large could be carried out, keeping terms of order  $\rho^{5/2}$  in H, but that a higher order correction must be added to (16) (to determine  $\tan^3 \bar{\Phi}_s$  terms which drive the  $\nu_0 = \frac{1}{5}$  resonance).

D. Computations and Large Amplitude Phenomena

A computer program (MURA Program F151), described in Ref. 1, was used to test the preced-

ing theories and to examine large amplitude motions (and questions of stability) not completely determined by the theories. Previously, for fixed  $\Gamma$ , ( $\Gamma = 0.5$ ) variation of  $\nu_0$  was studied (Figs. 3, 4, and 6-8 of Ref. 1). The present computations have involved varying  $\Gamma$  near resonances, particularly the intrinsic 1/3 and 1/4 integral resonances.

Near the resonance  $\nu_0 = \frac{1}{3}$  ( $N = 1$ ), resonant effects simply aren't confined to small amplitudes, unless  $\Gamma \ll 1$ . Figure 1 shows the strong dependence of large amplitude stability on  $\Gamma$ . Figures 1A and 1B indicate the change that occurs even without the resonance, and 1C shows the existence of a stable bead structure for  $\Gamma = 0.3$ . In general, however, for values  $\nu_0 > \frac{1}{3}$ , even small- $\Gamma$  beads become islands as  $\nu_0$  is increased. This happened (not shown) around  $\nu_0 = 0.36$  for  $\Gamma = 0.3$  and  $0.39$  for  $\Gamma = 0.1$ , for the parameters we used (which involve minimum conceivable values of the adjustable parameter  $h$ , and largest Rf voltages  $\frac{V}{E_S}$ , where  $V/E_S = 0.030$  the most unfavorable case for stability). For  $\Gamma \leq 0.5$  large amplitude stability is present at  $\nu_0 = \frac{1}{3}$  where small amplitudes are unstable, so that particles could be brought through the resonance from  $\nu_0 > \frac{1}{3}$  to  $\nu_0 < \frac{1}{3}$  with high efficiency. For  $\Gamma > 0.5$ , this is not true (even the "propeller" is unstable). For either case, phase space dilution would be very great for particles that survived. Conversely, only a small fraction of the beam could survive a passage upward through the resonance even for low values of  $\Gamma$ .

For the intrinsic quarter-integral resonance, the situation is less pessimistic. Figure 2 shows that bead positions change between  $\Gamma = 0.3$  and  $0.5$  indicating that the predicted null in the resonance lies between them, rather close to  $0.5$  in the lower frequency case (it was about equidistant for  $\nu_0 = 0.272$ ). Thus, in passing through this resonance values of  $\Gamma$  around  $0.4$  seem advisable (slightly lower for higher  $\nu_0$ ), or one might possibly avoid any effects by suitably programming  $\Gamma(\nu_0)$ . Large values of  $\Gamma$  caused instability, however, as Fig. 2D indicates, for  $\Gamma = 0.7$ .

In calculations with symmetrically placed accelerating gaps ( $N = 5$ ; see for instance Figs. 7 and 8 of Ref. 1) the half- and third-integral imperfection resonances become quite manageable and the one-fourth integral resonance becomes negligible.

E. Conclusions

The use of Moser transformations has been

seen to generalize our original theory so as to make correct qualitative predictions for all of the small to medium amplitude resonance phenomena so far studied.

We have investigated the  $\Gamma$  dependence of the one-third and one-fourth resonances in an  $N = 1$  system and find that except for very small  $\Gamma$ , the third-integral resonance is disastrous, but that the effects of the quarter-integral resonance may be minimized. In particular, if  $\Gamma$  is to be held constant as  $\nu_0$  is varied, a value of  $0.3$  to  $0.4$  for  $\Gamma$  renders resonant effects minimum. In an accelerator with many (we used  $N = 5$ ) symmetrically placed accelerating gaps, however, the one-fourth, one-third, and even half-integral resonances cause relatively small perturbations.

In any practical device for acceleration (i.e. not including stationary bunching applications of an RF system) in which one plans to cross the resonance  $\nu_0 = \frac{1}{3}$  in an upward direction or operate with  $\nu_0$  significantly greater than one-third, we have shown that two or more accelerating gaps (symmetrically placed) are necessary.

References

1. Symon, Steben, Laslett, Proc. of Int'l. Conf. on High Energy Accelerators (Frascati, 1965). To correct typesetting errors in this reference, substitute  $\epsilon$  for  $E$  in Eq. (2.13) and in every equation after (3.1).
2. Moser, Nachr. Akad. Göttingen, Math-Physik Kl IIa, 6, 87 (1955).
3. Symon and Sessler, Proc. of Symp. on High Energy Accelerators (CERN, 1956), Vol. 1, p. 44, give  $\alpha_3(\Gamma)$ .
4. Birkhoff, Dynamical Systems, Amer. Math. Soc. (New York, 1927), Vol. IX.
5. Courant and Snyder, Ann. Phys. 3, 1 (1958); see Appendix of present paper.
6. Hagedorn, CERN 57-1 (1957).

Appendix

Floquet Functions for Synchrotron Oscillations

The matrix<sup>5</sup> for transformation through one revolution is given by

$$M(\tau) = \begin{bmatrix} \cos \sigma + \alpha \sin \sigma & \beta \sin \sigma \\ -\gamma \sin \sigma & \cos \sigma - \alpha \sin \sigma \end{bmatrix}^N \quad \begin{aligned} \sigma &= \frac{2\pi\nu_0}{N}, \quad \alpha = \frac{(1-i)}{2} \frac{2\pi\nu_0^2}{\sqrt{\cos(\sigma/2)}}, \quad f = 1 - \frac{\gamma}{2\beta} \\ \beta &= \frac{1 - (\frac{e^2 N^2}{4\pi}) f(1+f)}{\nu_0 \sqrt{\cos(\sigma/2)}}, \quad \gamma = \frac{\nu_0^2}{\sqrt{\cos(\sigma/2)}} \end{aligned}$$

The linear transf. to c.o. coordinates  $\mathfrak{S}$  and  $\mathfrak{Z}$  is given by

$$\varphi = \sqrt{\frac{\beta}{2}} \begin{bmatrix} e^{i\chi} \mathfrak{S} + e^{-i\chi} \mathfrak{Z} \\ y = i \sqrt{\frac{2}{\beta}} \left[ (1-i\alpha) e^{i\chi} \mathfrak{S} - (1+i\alpha) e^{-i\chi} \mathfrak{Z} \right] \end{bmatrix}$$

where  $\beta_0 = (\beta \text{ evaluated at } \tau=0)$  and

$$\chi = -\frac{\pi}{2} + \int_0^\tau \left( \frac{1}{\beta(\tau')} - \nu_0 \right) d\tau' \xrightarrow{\nu_0 \rightarrow 0} -\frac{\pi}{2}$$

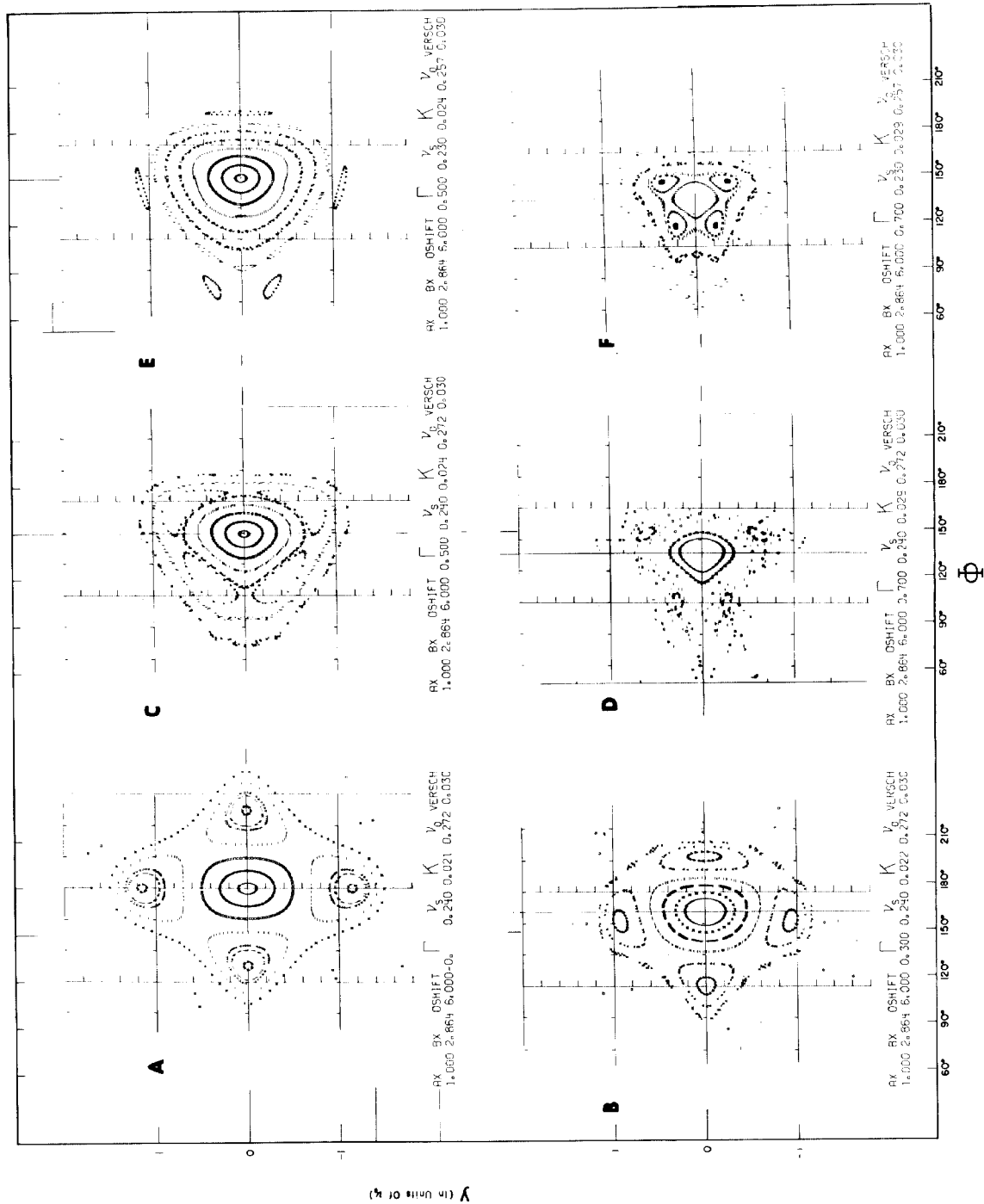


Fig. 1. Variation of phase areas with  $\Gamma$  at intrinsic  $\nu_0 = 1/3$  resonance.

- a.  $\Gamma = 0$  normal bucket,  $\nu_0 = 0.02$
  - b.  $\Gamma = 0$ ,  $\nu_S = 0.28$ ,  $\nu_0 = 0.35$
  - c.  $\Gamma = 0.3$ ,  $\nu_S = 0.28$ ,  $\nu_0 = 0.35$
  - d.  $\Gamma = 0.5$ ,  $\nu_S = 0.275$ ,  $\nu_0 = 0.333$
  - e.  $\Gamma = 0.6$ ,  $\nu_S = 0.275$ ,  $\nu_0 = 0.333$
  - f.  $\Gamma = 0.8$ ,  $\nu_S = 0.275$ ,  $\nu_0 = 0.333$
- Scale in d through f is magnified.

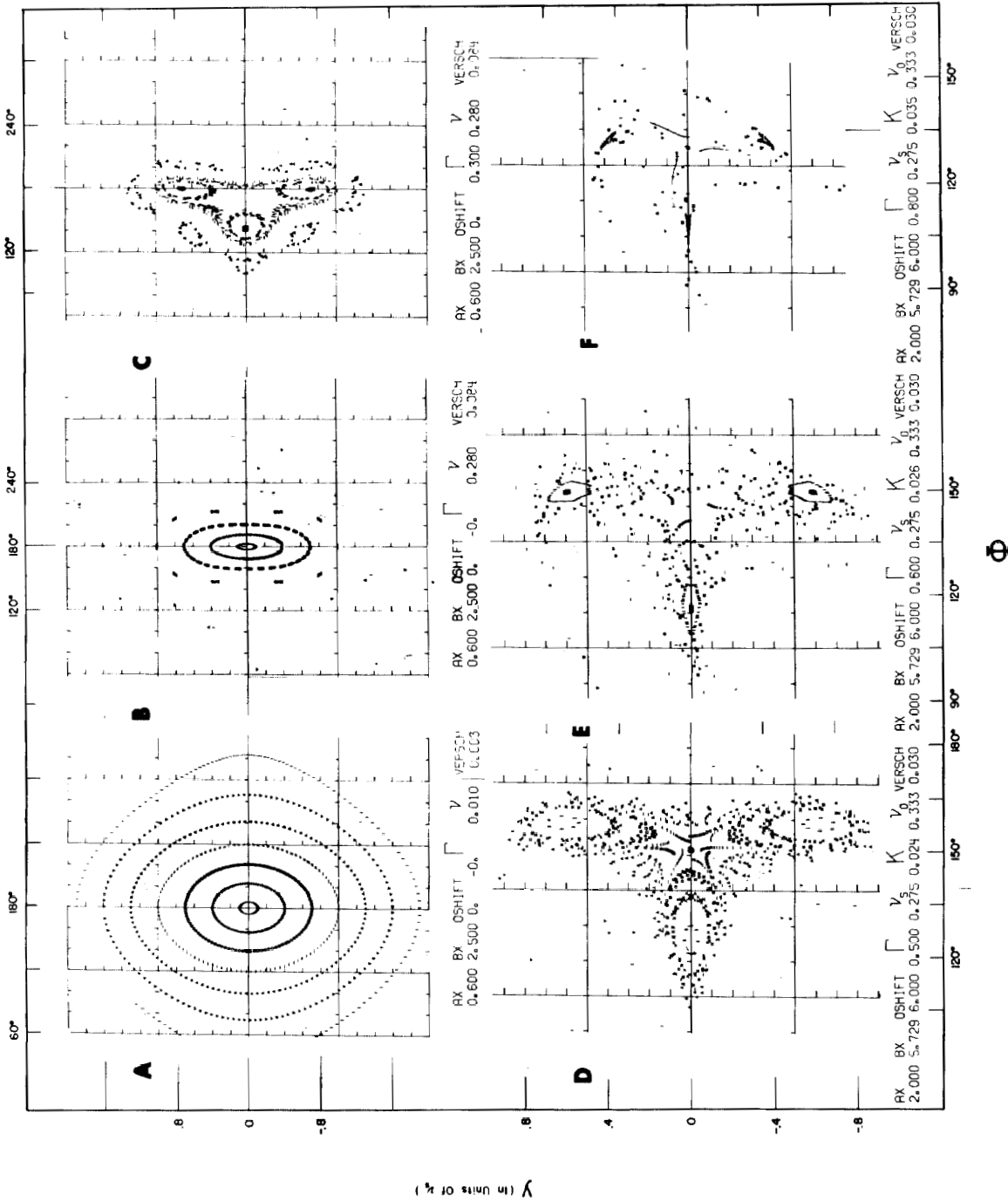


Fig. 2. Variation of the quarter-integral resonance as a function of two frequencies.

- a.  $\Gamma = 0, \nu_S = 0.24, \nu_O = 0.272$
- b.  $\Gamma = 0.3, \nu_S = 0.24, \nu_O = 0.272$
- c.  $\Gamma = 0.5, \nu_S = 0.24, \nu_O = 0.272$
- d.  $\Gamma = 0.7, \nu_S = 0.24, \nu_O = 0.272$
- e.  $\Gamma = 0.5, \nu_S = 0.23, \nu_O = 0.257$
- f.  $\Gamma = 0.7, \nu_S = 0.23, \nu_O = 0.257$